Characterization of tunneling cracks in Al_2O_3/Al_2O_3 +3Y-TZP multilayered composites by Raman and fluorescence piezo-spectroscopy

GOFFREDO DE PORTU, LORENZO MICELE
National Research Council, ISTEC-CNR, Faenza, Italy/Research Institute for Nanoscience, RIN

GIUSEPPE PEZZOTTI
Research Institute for Nanoscience, RIN, Kyoto Institute of Tecnology, Sakyo-ku, Matsugasaki 606-8585, Kyoto, Japan

In ceramic multilayered composites, consisting of layers of different composition, residual stresses are generated by different sintering strain rate between layers [1, 2] and thermal expansion mismatch between the layers during cooling down from sintering temperature [1, 2]. In Al_2O_3/Al_2O_3+3Y-TZP multilayered composites, layers with the lower thermal expansion coefficient (CTE), i.e. Al_2O_3 (A), undergo compressive residual stress while tensile stress appears in Al_2O_3+3Y-TZP (AZ) layers with higher CTE. This stress field directly affects the mechanical properties of the composites and it is responsible for cracking and/or delamination. In addition, spontaneous cracking upon cooling is sometime observed as a result of different sintering strain rate and excessive mismatch in CTE between layers. The processing defects analyzed in this paper are tunneling cracks in the AZ layers, spontaneously propagated upon cooling perpendicular to layer interfaces, while in a companion paper delamination cracks will be examinated. All defects were characterized measuring the stress field and the percentage of monoclinic ZrO_2 in their neighborhood.

The stress distribution field around tunneling cracks was determined using piezo-spectroscopy techniques related to the chromophoric fluorescence of Cr^{3+} impurities in Al_2O_3. The principle of relating an observed line shift in a fluorescence spectrum to the state of stress has been described previously by Grabner [3]. When polycrystalline Al_2O_3 (having a fine grained microstructure and no significant texture) is subjected to a stress σ s the change in frequency $\Delta\nu$ in luminescence line is given by the tensorial relationship

$$\Delta\nu = \frac{1}{3}\Pi_{ii}\sigma_{jj} \tag{1}$$

where Π_{ii} is referred to as the piezo-spectroscopic coefficient (i.e., relating frequency to stress).

In multilayered composites, the constituent phases are subjected to two different kinds of stress fields: (i) a macroscopic (layer-to-layer) stress field, arising from the mismatch in CTE between different layers; and, (ii) a microscopic (grain-to-grain) stress field due to both difference (i.e., anisotropy) in CTE along different crystallographic axis in Al_2O_3 grains and between Al_2O_3 and ZrO_2 in composites. Upon elaborating data according to a method previously suggested by the present authors [4], it is possible to separate those two contributions. Using the "zero-stress" frequency and the Π_{ii} value obtained by the calibration of the pure A and composite AZ (Table I), respectively, the stress can be assessed through Equation 1. By doing so, the effect of microstress field on the experimentally determined spectral shift in the Al_2O_3 phase is automatically subtracted from the net measured shift. In other words, the Al_2O_3 phase can be used as a "stress sensor", because the shift of its spectral lines directly reads the macroscopic stress field piled up among the different layers of the structure.

To determine the fraction of monoclinic ZrO_2, the formula suggested by Katagiri *et al.* [5] was used:

$$X_{\text{mono}} = \frac{0.5(I_{177} + I_{186})}{2.2I_{144} + 0.5(I_{177} + I_{186})} \tag{2}$$

where I is the intensity of the band whose Raman shift (in cm^{-1}) is given in the subscript. According to Equation 2, it is possible to use the intensity of three selected bands of the ZrO_2 Raman spectrum to calculate the percentage of monoclinic ZrO_2 in the area probed by the laser beam. The presence of monoclinic ZrO_2 in 3Y-TZP around cracks is caused by stress-induced phase-transformation from the tetragonal to the monoclinic polymorph. Such a local phase-transformation phenomenon is the origin of a toughening mechanism exibited by ZrO_2-based materials.

Al_2O_3 and Al_2O_3 + 3Y-TZP (60/40 vol%) tapes were prepared as previously described [4, 6] and punched into 34 mm × 50 mm rectangles. Because the AZ layers are known to undergo tensile residual stress during manufacturing, the thickness of the AZ tape was selected higher than that of the A layer. An empirical assessment was made to obtain, after sintering, the desired thickness for AZ and A layers, respectively. In order to prepare laminates with different residual stress fields, the punched tapes were stacked to form two kinds of structure with different ratios between A and AZ thickness: (i) in the specimen henceforth referred to as A/AZ, 15 layers were stacked alternating A and AZ layers (180 ± 10 μm and 250 ± 10 μm

0022–2461

TABLE I Piezo-spectroscopic coefficients and stress-free band positions

Material	Stress-free value (cm^{-1})	Π_{R1} (cm^{-1}/GPa)
$Al_2O_3^*$	6084.16	−7.6
AZ 60/40 vol%**	6086.49	−6.9

Source: *[7], **[4].

in thickness, respectively) according to the sequence A/AZ/. . ./AZ/A; and, (ii) in the A/2AZ specimen, 13 layers (180 ± 10 μm and 500 ± 10 μm in thickness for A and AZ, respectively) were stacked according to the sequence A/2AZ/. . ./2AZ/A. To ensure rigid bonding between each stacked green sheet, warm pressing was carried out, prior to pre-heating and sintering, for 30 min at 80 °C, with a pressure of 30 MPa. Specimens were then placed in a low-temperature furnace up to 600 °C for a binder-burnout pre-heating cycle, with both heating and cooling rates of 3 °C/hr. The laminates were finally sintered at 1550 °C for 60 min with both heating and cooling rates of 30 °C/hr. Cross sections of the laminates (Fig. 1) were polished down to a 1 μm finish for optical and stereo microscopy observation.

Microscopic stress distributions were measured using fluorescence piezo-spectoscopic analysis. Either linear or two-dimensional arrays of spectra were collected around selected tunneling crack locations. Specimens were placed on an automatic mapping device (lateral resolution of 0.1 μm), which was connected to a personal computer to drive displacements of the probe on the sample surface. Both spot size and spacing between spectra collected at adjacent locations were comprised between 1 μm and 5 μm, depending on the spatial resolution desired. In this

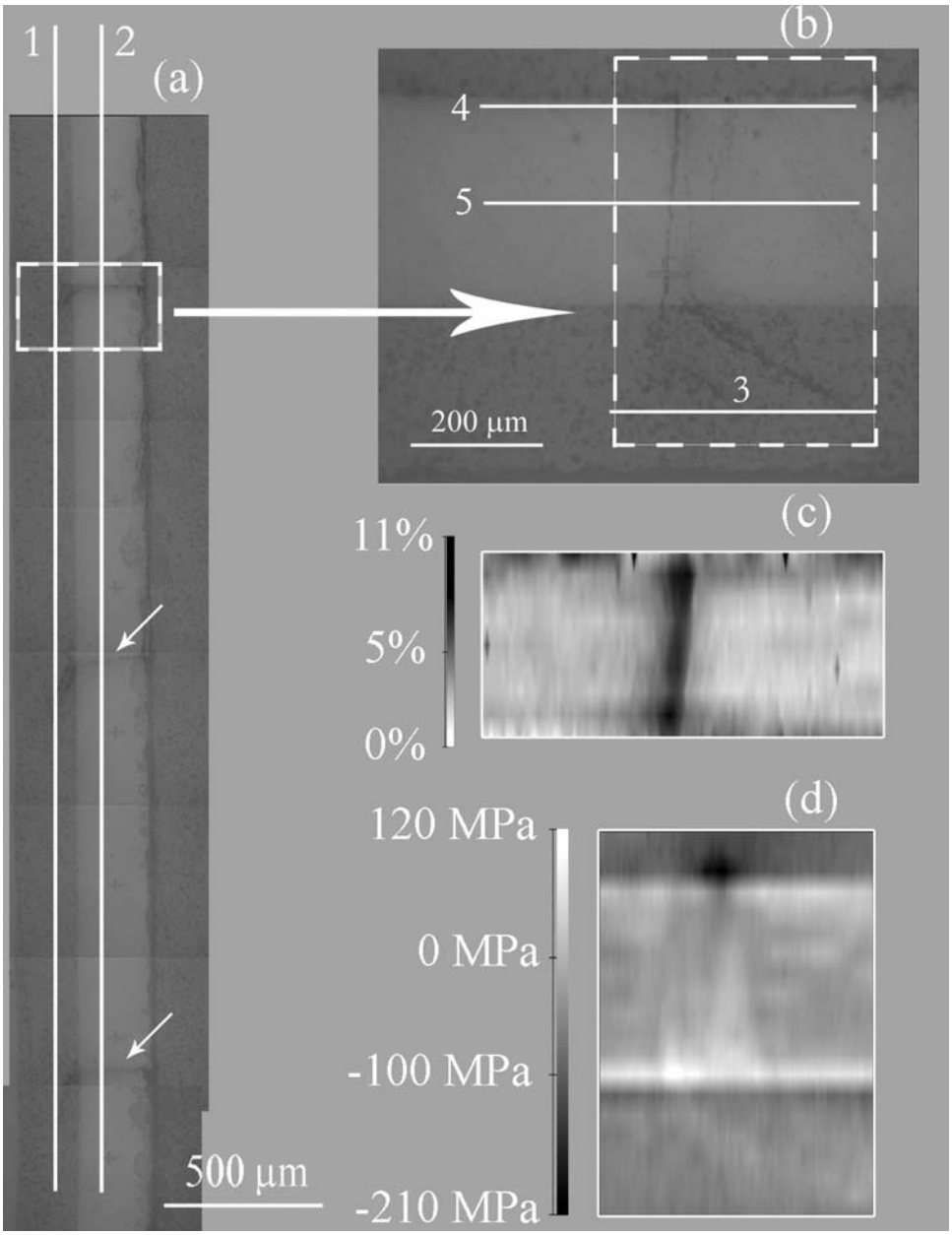

Figure 1 Micrograph of the whole analyzed area (a) and particulars (b) of crack on which stress and monoclinic fraction measurement were done. White lines represent the exact position of profiles to which the paper refers several times. (c) Map of distribution of m-ZrO_2, transformated around the crack path. (d) Macroscopic stress distribution in the area enclosed by the light blue area in Fig. 1b.

study, an optical microscope was used to both stimulate and collect the excited fluorescence, which was then analyzed using an attached spectrometer (T-64000, Horiba/Jobin-Ivon, Tokyo, Japan). An Ar^+ ion laser operating at a wavelength of 488 nm was used as the excitation source. For each map, the region of interest was first selected using the optical microscope. Then, spectra were collected using a CCD camera, integrating usually over 1 s for Al_2O_3 and 4–5 s for ZrO_2. As a reference fluorescence line for internal calibration, a commercially available Hg/Ne lamp was used. The collected data were subsequently analyzed with curve fitting algorithms (LabSpec 4.02, Horiba/Jobin-Ivon). Piezo-spectroscopic coefficients for both materials were taken from previously published work [4, 7], while reference band positions were collected from reference samples with the same composition and made by the same processing procedures except for lamination (i.e., free of macroscopic stress field). Piezo-spectroscopic coefficients for an equi-triaxial stress state and stress-free band positions are reported in Table I.

Fig. 1 shows a micrograph of the whole area analyzed by Raman spectroscopy (a) and a higher magnification image of a tunneling crack (b). A two-dimensional map is shown in Fig. 1c, which was collected over the entire thickness of the AZ layer, in the neiborhood of the crack path. This map illustrates the distribution of monoclinic ZrO_2 calculated using Raman spectrum of ZrO_2, according to (2). The map of Fig. 1d was collected using the chromophoric Al_2O_3 phase as a "stress sensor" therefore, the map represents the alteration of the macroscopic residual stress distribution field due to the presence of the crack in the area enclosed in the light blue rectangle of Fig. 1b. Tunneling cracks, perpendicular to layer interfaces, were only observed in AZ layers because they were under residual tensile stress. Cracks started from the A/AZ interface and propagated trough the AZ layer straight and then, when crossing the A layer, they usually bent and stopped in this layer, because crack-tip propagation was hindered by residual compressive stresses [8]. The three cracks present in the analyzed area were all very similar with regard to shape, dimension and spacing: They all split when entering the alumina layer. Whereas in previous studies [9–11] bifurcation was observed to occur simmetrically, here one tail became longer in all three cracks only the right tail continued within the A layer for 300–350 μm. This high simmetry and reproducibility may be due to the high homogeneity of the material. The laminate structure can re-distribute the stresses internally and survive to high stress without undergoing catastrophic fracture. The high simmetry of the material can be also confirmed in Fig. 2 whose plots refer to residual stresses measured along profile 1 and 3 of Fig. 1, within the A layer. The three maxima of the stress values in Fig. 2a represent the stress release in correspondence of the three crack paths. In Fig. 2b the profile of one of the three cracks is acquired with higher resolution across the crack path, where the residual stress goes to ∼0 MPa.

While in the A layer the stress release due to the presence of the crack path can be clearly envisaged, the stress profile acquired within AZ layer (Fig. 3a) only showed a decrease in the average value from a region far from the cracks (0 μm in the plot) toward the cracked area. In Fig. 3b, it is possible to observe a zone of compressive stress just near the A/AZ interface (line 4 in Fig. 1b). This zone (which corresponds to the crack path) is quickly recovered when the laser probe is moved toward the center of the layer. The different

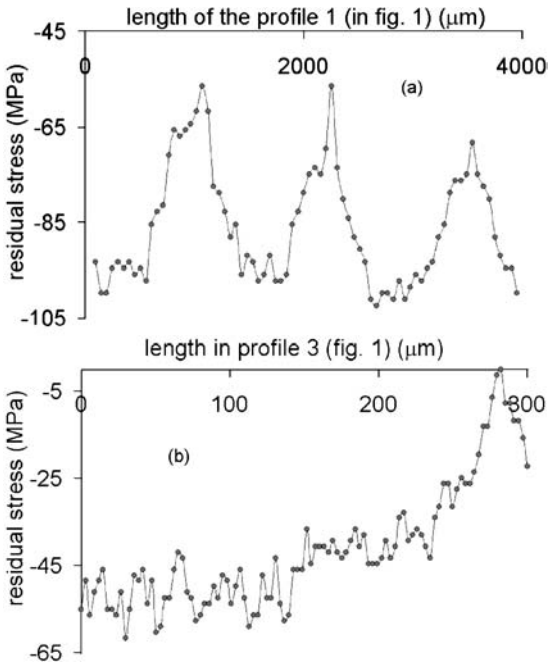

Figure 2 Residual stress in the cracked A layer: profile 1a and 3b in Fig. 1: the three peaks in (a) correspond to the release of stress in the neighbourhood of crack tip. (b) is a shorter profile with higher definition along line 3 of Fig. 1b.

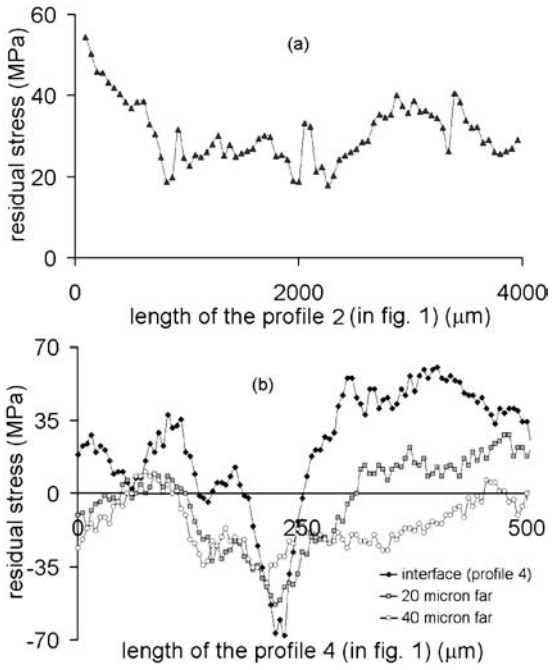

Figure 3 Residual stres in AZ cracked layer. Plot (a) is referred to profile 2 of Fig. 1a, in the center of the layer: on the contrary of A layer, no peaks are visible. Plots (b) are referred to profiles 4 and other two profiles acquired at 20 and 40 μm toward the center of the layer. The negative peak is in correspondence of the crack.

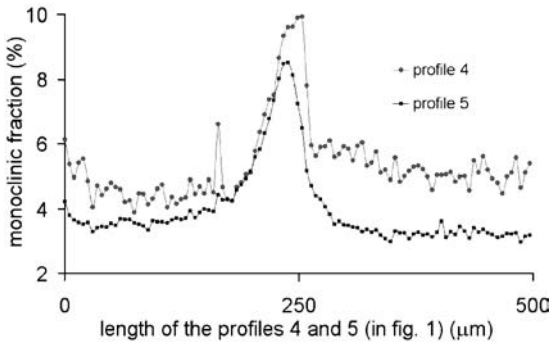

Figure 4 Monoclinic fraction across the crack (profiles 4 and 5). "Profile5" curve is the average of 7 profiles in the center of the layer, around the line numbered "5" in Fig. 1b. The peak around 250 μm is in correspondence of the crack.

behavior of AZ layer may be explained with the presence of a fraction of m-ZrO_2 phase around the crack paths, exactly in correspondence of the area undergoing high compressive stress. Infact, when a crack propagates throught ZrO_2, tetragonal-to-monoclinic transformation takes place. The crystallographic expansion ($\sim$4%) of m-ZrO_2 as compared to the tetragonal polymorph produces an additional stress field that alters the original residual stress status. In Fig. 4, the monoclinic fraction in the center of AZ layer is plotted and compared with that recorded close to the inteface. Both profiles, in correspondence of the crack, show a sharp peak with a two-fold fraction of m-ZrO_2, suggesting the activation of a toughening mechanism typical of 3Y-TZP. The higher fraction of m-ZrO_2 near the interface can easily explain the presence of a compressive stress field because of the crystallographic expansion of such a fraction of zirconia grains. On the other hand, in the center of the layer, the amount of m-ZrO_2 is systematically lower and it is not enough to annihilate the residual tensile stresses, but just reduces them from $\sim$60 MPa to $\sim$25 MPa (Fig. 3a).

Tunneling cracks in multilaminated alumina/alumina-zirconia composites were characterized using fluorescence piezo-spectroscopy of Al_2O_3 to measure residual stresses and Raman spectroscopy for the local (microscopic) determination of monoclinic ZrO_2 fractions.

A complete release of residual stresses was observed around crack paths in the A layers. The formation of m-ZrO_2 around cracks in AZ layer affected the residual stress distribution according to the amount of transformed phase. In the AZ layer the volume fraction of m-ZrO_2 around the cracks close to the interface was relevantly higher than in the center. As a consequence, in areas close to the interface the stress became compressive while in the center of the layer remained tensile in nature, even if a remarkable amount of its magnitude was released. The presence of partially stabilized (and thus transformable) t-ZrO_2 in the AZ layers under residual tensile stress is effective in reducing the residual stress field and thus in hindering crack propagation. This significantly contributes to improve the structural performance of laminated composites.

References

1. P. Z. CAI, D. J. GREEN and G. L. MESSING, *J. Amer. Ceram. Soc.* **80** (1997) 1929.
2. T. CHARTIER, D. MERLE and J. L. BESSON, *J. Eur. Ceram. Soc.* **15** (1995) 101.
3. L. GRABNER, *J. Appl. Phys.* **49** (1978) 580.
4. G. DE PORTU, L. MICELE, G. PEZZOTTI and Y. SEKIGUCHI, submitted to *Acta Mater.*, September 2003.
5. G. KATAGIRI, H. ISHIDA, A. ISHITANI and T. MASAKI, Advances in Ceramics, in Science and Technology of Zirconia III (Vol. 24A), edited by S. Somiya, N. Yamamoto, H. Yanagida (The American Ceramic Society, Westerville, 1988) p. 537.
6. M. JIMENEZ-MELENDO, C. CLAUSS, A. DOMINGUEZ-RODRIGUEZ, G. DE PORTU, E. RONCARI and P. PINASCO, *Acta Mater* **46** (1998) 3995.
7. J. HE and D. R. CLARKE, *J. Amer. Ceram. Soc.* **78** (1995) 1347.
8. P. Z. CAI, D. J. GREEN and G. L. MESSING, *J. Eur. Ceram. Soc.* **18** (1998) 2025.
9. M. P. RAO and F. F. LANGE, *J. Amer. Ceram. Soc.* **85** (2002) 1222.
10. M. OECHSNER, C. HILLMAN and F. F. LANGE, *J. Amer. Ceram. Soc.* **79** (1996) 1834.
11. A. J. SANCHEZ-HERENCIA, L. JAMES and F. F. LANGE, *J. Eur. Ceram. Soc.* **20** (2000) 1297.

Received 25 May
and accepted 9 July 2004